TEST BEAMS FROM THE HEB

T. Kirk

Fermi National Accelerator Laboratory, P. O. Box 500, Batavia, IL 60510

Introduction

The SSC detectors during their construction period will require extensive use of test beams containing particles ranging from a few GeV to several TeV. The existence of the High Energy Booster (HEB) allows the production of flexible and high duty factor test beams with energies ranging from a few GeV up to 1 TeV. In this paper, a conceptual design is put forward for such a test beam facility. The remaining applications for which particle energies above 1 TeV are needed in the test program is not addressed here; other contributions to the summer study address these needs[1].

Of particular interest in this regard is the interesting plan from Timothy Toohig and Mike Harrison for combining the beams from the HEB developed in this paper with beams of 20 TeV (machine energy protons) and 20 TeV neutrons from an interaction point in a common experiment building and test facility. These combined beams plans will address most of the presently envisioned test beam needs of the experimental program. Since the details of primary beam routing are not fully developed at this writing, the present design will concentrate on the target system and secondary beam properties of the test beams derived from the 1 TeV HEB primaries. Details of the 1 TeV primary beam transport remain to be worked out to complement the 20 TeV proton test beam as noted above. As an existence proof for the 1 TeV primary beam, a specific transport is developed here assuming an extracted beam of likely phase volume[2].

Finally, it is noted that the present design generally follows the conceptual plan for HEB test beams as presented in the SSC Conceptual Design Report SSC - 2020[3]. The present design, however, elaborates on the CDR plan and provides detailed estimates of beam yields and emittences for various primary and secondary beam configurations. The most significant capability advanced in this paper beyond what was presented in the CDR is the use of target-angle dipoles just upstream of the target stations. These dipoles permit different secondary energies to be chosen in each branch of the dual beams that emerge from the target stations. This new degree of flexibility seems a useful advantage for the envisioned test beam program.

Basic Design Philosophy

For very high energies, particle test beams can be reduced to a small number of types: hadrons; electrons; muons; photons. Charged hadron beams have the advantage over neutral ones that momentum tagging and particle ID can usually be added across most or all of the energy spectrum. Likewise, electrons can be tagged prior to use over a significant part of the energy spectrum by the use of TRD detectors and/or purified by separation from equal momentum charged hadrons using synchrotron radiation or by repeated charged to neutral to charged beam conversion. Finally, muons can be post-tagged by their penetration through thick iron or earthen absorbers after being used in the test setup.

In this paper, we develop a plan for charged particle beams at or below 1 TeV using magnetic transports with good optical properties, zero-degree particle production angles and flexible energy and intensity characteristics. The special tricks needed to produce high quality or high purity electron beams are not developed here.

Basically, then, we develop a plan that will produce four charged-particle test beams having good duty factors, adequate intensity and good energy flexibility, while staying within parsimonious cost levels and retaining simplicity of operation and maintenance. The latter criteria derive from general SSC conceptual design guidelines and cost estimates as they appear in the CDR. The four test beams come from two primary proton target stations, each of which receives a 1 TeV primary proton beam from the HEB. The protons which come to each target station are regarded as coming from a switched primary beam with 0-100% duty factor (one beam runs while the other is off, a necessary result of the switching mode of proton sharing). If test beam use rises to a critical level, the HEB primary beam could be split rather than switched to provide double the original duty factor. This involves additional cost and complication, but no new conceptual advances.

Each of the two primary beams has a set of quadrupole focussing magnets and a set of incident-angle-varying dipole magnets upstream of the primary target plus a set of dipole sweeping magnets just downstream of it (Fig. 1). The production target and sweeping dipoles are enclosed in a steel radiation shielding vault which is located in an underground target enclosure for further radiation shielding protection (Fig. 2). At the downstream end of the target vault is a water-cooled aluminum beam dump with two symmetrically placed holes through which the charged secondary beams pass to become the test beams.

The magnetic geometry of each of the two target stations, including their incident-angle-varying dipoles results in the circumstance that each of the two secondary beams from a particular target station will have the opposite electric sign of the other beam from that station (Fig. 2). It might at first seem that requiring the beams to be of opposite electric sign is a severe constraint to place on two supposedly independent test beams. Indeed, except for the fact that they are explicitly beams for testing apparatus, not carrying out particle research, it would be a significant constraint. When testing at high energy, however, the sign of the test particle is irrelevant most of the time; only its type and energy are relevant. Because the secondary beams are totally charge symmetric, any particular test need can be met for one of the two beams; the other is then constrained to use opposite sign particles.

The HEB accelerator is not a rapid cycling machine, but it is capable of delivering slow spill beam over a period of minutes once the internal beam has been accelerated to 1 TeV. In this way, a good duty factor can be realized by sustaining several minutes of

slow spill for each 65 second acceleration cycle. Stretching the 10^{13} or so protons over a spill several minutes in length places a premium on efficient collection and transport of secondaries, even in a test beam. As a result, the design adopted here is organized so that 0° production is always used for the test beam secondaries as well as a solid angle size chosen to collect an appreciable fraction of the full transverse momentum spectrum at production (especially for the highest momentum tunes). Likewise, since a secondary beam optimized for energies comparable to the incident energy is not efficient for collection and transport of particles of much lower energy, a retarget scheme is incorporated to produce test beams (when needed) that range from 0.5% to 15% of the primary energy (5 GeV to 150 GeV). This tertiary beam can be made quite intense by transporting primary-energy diffracted protons to the downstream production target and collecting the low energy beam products there.

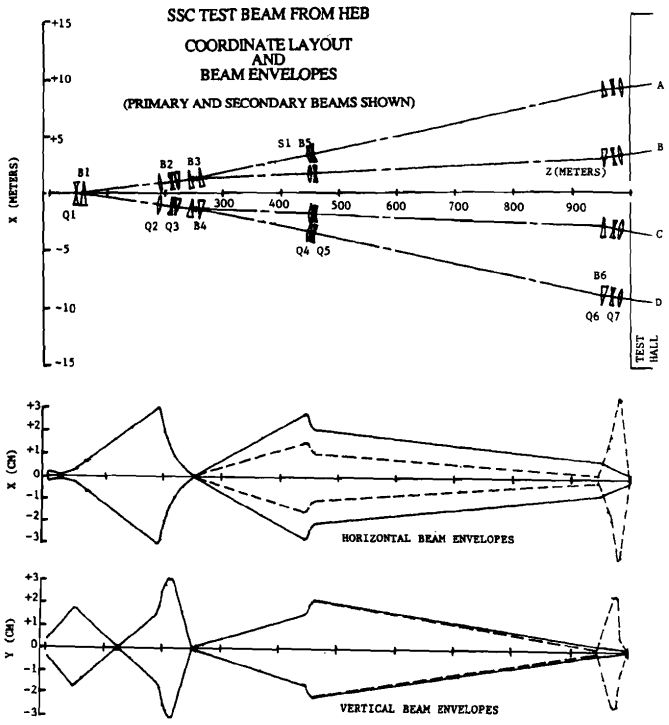

Fig. 1 - HEB Derived Test Beam schematic layout and beam envelopes. The dashed lines indicate low energy tunes produced by refocussing diffraction scattered 1 TeV primaries from the first target onto the second.

In the case of the high energy test beams (150 - 1000 GeV), care was taken to produce an achromatic beam transport that has an appreciable momentum bite when the full aperture is selected, this while maintaining a good final focus (hence small spot size) at the end test station. The achromiticity property could not be maintained in the low energy configuration, but the spot size is still manageable as will be seen (Figs. 4,5). The desire to maintain a large momentum acceptance for the beam is connected directly with the desire to maintain reasonable intensities even in the long spill mode described above.

Transmitting a large mommentum bite can, of course, cause its own problems. Chief among these (in a test beam especially) is the fact that a typical end-use job for the beam is to measure the energy resolution of a detector under test. When the beam momentum spread is large (or comparable) to the detector resolution, special measures must be taken. In contemporary setups, the answer is often to use a beam tagging system (usually based on wire chambers and a bending dipole) that can measure with high precision (typically 0.5% or so), the precise trajectory of each relevant beam particle. The beam momentum is thereby obtained on a particle by particle basis for comparison with the detector response. This approach is used in the present design for the high energy beams and is known to be workable with raw beam intensities up to 10^8 sec^{-1}. For the low energy tune, the beam momentum is derived from particle trajectories through the capture quadrupoles rather than through tagging dipoles, but the reconstruction principles are the same.

The subject of beam particle ID is not developed here, but the methods are well known and can be applied as needed to the offered beam geometry. To catalogue all the different possible cases is more the subject of a monograph than a summer study paper, so we skip over this topic. Instead, we continue with a technical description of the test beam design.

Primary Beam Transport and Targeting

Figure 1 shows a scaled schematic view of the primary beam transport from the HEB to the two primary target stations. As noted in the Introduction, the desire to incorporate 1 TeV HEB-derived and 20 TeV Main-Ring-derived test beams in a single test building will influence the disposition of the HEB primary transport on the SSC-site and probably modify its optics to some extent as well. For this reason, we show in Fig. 1 mainly aspects of the transport associated with switching 1 TeV protons between the two production targets (B1 dipoles), target focussing (Q2, Q3 quadrupoles) and incident-angle-varying (B2, B3 dipoles) elements.

Regardless of the macroscopic site layout, the juxtaposition of the two target stations and the proton switching geometry will likely remain unchanged. The reasons for this will become clear shortly. Small trim dipoles for vertical steering are left out of the drawing. In an engineering design, these would be needed and placed in appropriate locations.

Before discussing the optics and beam transport strategy, a brief word on magnets is useful here. The entire design is based on existing conventional iron-copper magnets of types which have been used successfuly for years for primary beam transport at Fermilab. The idea is to design on the basis of known, practical magnet designs, thereby insuring the buildability of the resulting beam transport concepts. Of primary interest here is the explicit choice of conventional rather than superconducting magnets. The reliability, ease of use and freedom from complication of such magnets in external beam transports with small bending angles has been proven at Fermilab in the TeV II fixed target areas.

The specific dipole chosen is the so-called 'EPB dipole', a water cooled laminated iron magnet of length 10 feet, with clear vacuum aperture of 1 inch x 5 inches and maximum field of 1.5 Teslas at 1700 amperes. The quadrupole chosen is the so-called '3Q120 quadrupole', a water cooled laminated iron quadrupole of 10 foot length and 3 inch diameter clear aperture with a maximum gradient of 20 Tesla/meter at 100 amperes. Being made of laminated iron, both magnets can be ramped to full field in a few seconds and polarity reversed (with appropriate power supplies and switches). This feature is used in the B1 switching scheme. We proceed assuming these magnets are used at each point in the transport.

We assume for the conceptual design purposes, a primary beam exiting the HEB driven by a half-integer resonant slow extraction system similar to the Fermilab Tevatron[2]. Like that beam, the emittence properties will be governed by the extraction process, not by the emittence of the circulating beam. For specificity, we assume the following properties of the extracted beam:

Table I
Properties of 1 TeV Extracted Beam from the HEB

horizontal emittence	.03 mm mr (95%)
vertical emittence	1.0 mm mr (95%)
spill rate	10^{13} protons/5 minutes
rf bunching factor	±0.2 ns/16ns (95%)
energy spread	1.0×10^{-4} ΔP/P

The extracted beam is phase-matched to the primary beam transports by Q1 which is placed just upstream of the switching dipole B1. The dipole then switches the primaries to one or the other target station by bending them through angles of ±6.75 mr. Each beam then proceeds to its own production target at Z=250M and X=±1.3M. The protons are focussed onto the production targets by pairs of quadrupole doublets Q2, Q3 in each beam.

In order to achieve the desired goal of decoupling the momentum of the secondaries in each of the two transports coming from a single target station, the primary proton beam is brought in at a variable angle and correlated transverse target position. Varying the incident angle and primary target position plus varying the secondary beam bending with a common sweeping magnet downstream of the production target, allows the secondary beams to have different energies. The beam transport result is shown in Fig. 2 for a tune of P1=+1000 GeV/c and P2= -200 GeV/c. This particular tune is near an extreme of the required angle varying conditions. The angle-varying bends are accomplished with dipoles B2 and B3.

In Fig. 4 the required bend angles in B2, B3 and B4 and the necessary associated target position spatial offsets are shown for variable ratios of the secondary momenta (R= |P1/P2|). Note that either secondary beam can have the positive electric charge and that either beam can have the higher energy. In practise, an important configuration will be that for which one beam is tuned to primary beam energy (1 TeV) but away from 0° so that diffraction scattered protons of a selected intensity can be transmitted to the second target, while variable energy negative beams (150 - 1000 GeV) are used in the other transport. To avoid complication, the graphs in Fig. 4 are given only for 0° secondary production, but it is straight forward to develop the magnetic conditions for variable transverse momentum of the secondary beams. This is not included here, but in a real design the secondary beam production angle will be another highly useful parameter for controlling the compatibility of the two test beams.

The beam envelope for the assumed primary proton beam is shown in Fig. 1 and the magnet parameters are shown in Table II.

Table II
Primary Beam Magnet Parameters (1 TeV)

Magnet	Aperture(cm²)	Length (M)	Field(kg;kg/cm)
B1	2.5 x 12.0	5 x 3.0	±15.0
B2	2.5 x 12.0	2 x 3.0	0.0 - ± 15.0
B3	2.5 x 12.0	5 x 3.0	0.0 - ± 15.0
Q1	7.2 D	2 x 3.0	-1.69
Q2	7.2 D	2 x 3.0	+2.09
Q3	7.2 D	3 x 3.0	-2.11

The primary 1 TeV beam as assumed can be focussed to a circular spot of diameter 0.05 cm (95%) on the production target. This spot is, of course, decoupled from the target angle-varying system.

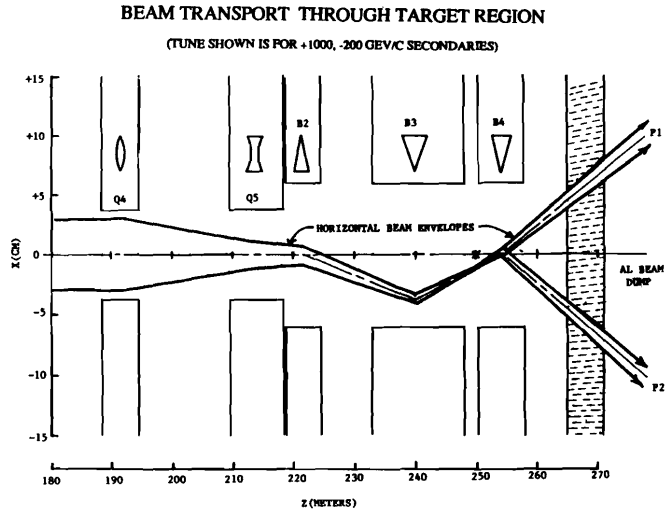

Fig. 2 - Details of the angle-varying dipole system for independent momentum selection in the two secondary branches of the upstream target stations.

Primary Target Stations

The primary target stations are located side by side in a common underground target enclosure. It is assumed that they will be enclosed in a steel radiation containment vault to protect groundwater and reduce radiation exposure to service personnel from residual target area radioactivity after extended periods of operation. By arranging that the two target stations are separated by 2.6 M, a practical servicing geometry and compact enclosure properties are assured. More on these subjects later.

The primary targets are located within the target vaults. Just downstream of each target is a pair of special target sweeping dipoles of a type developed at Fermilab for this application (B4). These dipoles are constructed of radiation - hard materials and are used to sweep the secondary beams into the secondary beam magnetic transports. The transports are begun by symmetrically placed apertures in the water-cooled aluminum beam dump that terminates the target stations. As designed, these apertures will be about 1.0 cm x 1.0 cm each at their downstream ends and subtend a solid angle of 0.23 μsr at the targets. This is equivalent to a transverse momentum acceptance of 0.19 GeV/c at 800 GeV secondary energy, a good fraction of the central production peak. Less transverse momentum is accepted at lower energies, but particle production increases rapidly with decreasing energy so the fluxes should be adequate (Fig. 6).

The magnetic field in the sweeping magnet B4 depends on the desired momenta P1 and P2 in the secondary beam transports. In Fig. 3, the value of θ(B4) is shown for the important case where P1 = 1000 GeV. Lower values of P1 for variable R are just scaled linearly down from this curve.

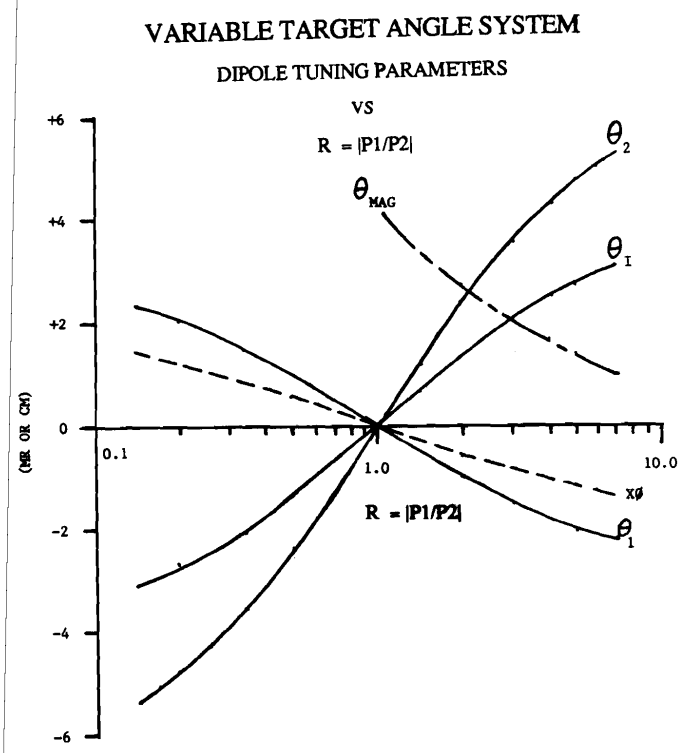

Fig. 3 - Parameter values for target position and dipole angles for the angle-varying target system as a function of the ratio of secondary beam momentum values.

One last subject to note in this section is the question of radiation safety for the case of beam transports which have the ability to carry machine energy beams into inhabited buildings (the Test Hall). In the design presented, the magnets have an adequate parameter range to carry 10^{13} primary beam protons into the Test Hall. This has been the situation over the years for several beams at Fermilab also. To prevent this possible occurance from ever actually happening, fail-safe, redundant controls and protection methods have been developed to prevent tunes which can produce the result of 10^{13} beams into the Test Hall. It is beyond the scope of this paper to develop such a plan, but we note here the need for and practically of such a protection system. Such systems are usually based on secure-systems controlling the power supplies for the relevant beam transport magnets.

High Energy Secondary Beam Transport

The transport of high momentum secondary beams is also shown in Fig. 1. There it is seen that the spatial separation of the four test beams is determined by the dipoles B4, B5, B6 and the optical properties by the quadrupoles Q4, Q5. Intensity is controlled primarily by a variable-aperture beam collimator located just in front of quadrupole Q4. The aperture of this collimator (S1) also controls the momentum acceptance of the secondary beam due to the dispersive effect of the target sweeping magnet B4.

Momentum tagging of the high energy secondaries is accomplished by use of planes of 1mm-pitch multiwire proportional chambers (MWPCs) arranged upstream and downstream of the dipole B6. This magnet has a bending angle of 4.725 mr, which would allow tagging precision of $\sigma(\Delta P/P)$=0.6% with 20M lever arms before and after the magnet. As designed, the tagging system and the final beam transport elements B6, Q6, Q7 are housed in underground tunnels of approximate length 60M leading into the Test Hall at its upstream end. Spaces between the tagging stations and transport elements could be used to accommodate particle ID devices such as TRDs and DISC counters.

The final quadrupoles Q6, Q7 are not needed for the high momentum tunes (they are for test beams below 150 GeV), but could be used for special tunes in a test program. The high energy secondary beam magnet parameters are given in Table II and the beam envelopes are displayed as solid lines in the lower part of Fig. 1. The detailed spot size and momentum distribution were calculated by the ray-tracing program TURTLE[5] with the slit width S1 set at 3.0 cm (nearly fully open) and actual magnet apertures. The results are displayed in Figure 4.

Table III
High Energy Secondary Beam Transport (+800 GeV)

Magnet	Aperture(cm²)	Length (M)	Field(kg;kg/cm)
B4	2.5 x 12.0	2 x 3.8	±14.40[1]
B5	2.5 x 12.0	3.0	+ 2.08
B6	2.5 x 12.0	3 x 3.0	-14.00
Q4	3.8 D	2 x 3.0	- 1.11
Q5	3.8 D	2 x 3.0	+ 1.06

[1]A symmetric tune of ±800 GeV is assumed here.

Secondary Target Station and Low Energy Beams

For secondary beam energies below 150 GeV, it is more efficient to produce the particles at the secondary beam target stations located just before dipoles B6. In this circumstance, the B6 dipole acts as a target sweeping magnet and secondary beam momentum selector. Quadrupoles Q6, Q7 collect the secondaries from the target and focus them into the test apparatus.

To produce the most intense low energy beam fluxes, a beam of diffracted protons from the primary beam target station is transported to the secondary beam target and focussed onto this target using Q4, Q5. Even though these magnets are far from the target, spot sizes of 0.17 cm x 0.09 cm can be achieved. These spots are small enough for satisfactory secondary beam production. In certain circumstances, it may be desireable to transport secondaries from the first target to the second for production of low energy tertiaries. The dashed beam envelopes in Fig. 1 show the transport of diffracted protons to the second target station and the capture of low energy tertiaries from this station plus their transport to the Test Hall. The magnet transport parameters are displayed in Table IV.

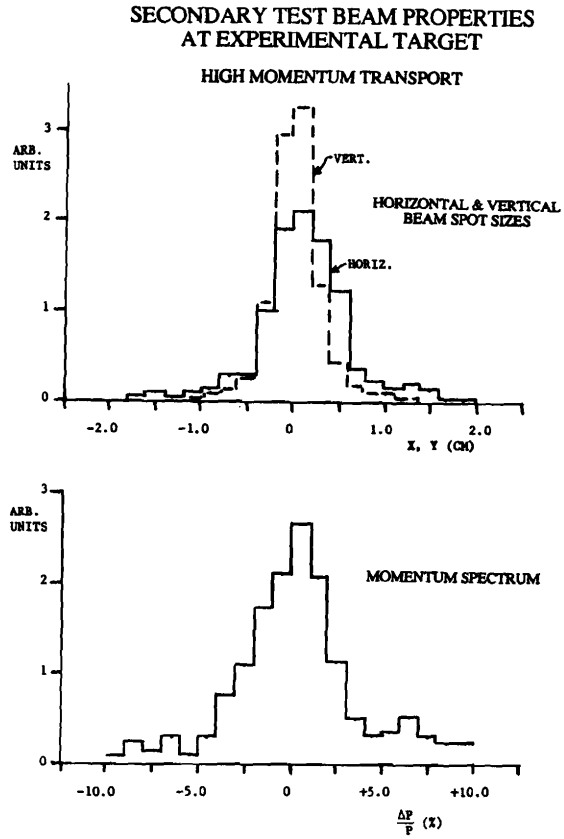

Fig. 4 - Beam spot size and momentum spread at the Test Hall for the high momentum test beam transport.

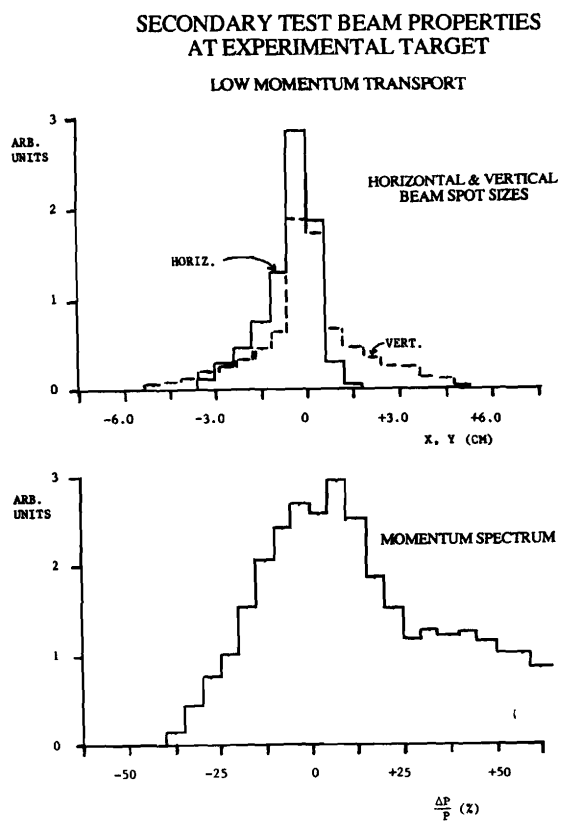

Fig. 5 - Beam spot size and momentum spread at the Test Hall for the low momentum test beam transport.

Table IV
Magnet Parameters for Tertiary Test Beam (+150 GeV)

Magnet	Aperture(cm²)	Length (M)	Field(kg;kg/cm)
B4	2.5 x 12.0	2 x 3.8	+ 6.00[1]
B5	2.5 x 12.0	3.0	+ 2.60
B6	2.5 x 12.0	3 x 3.0	- 2.63
Q4	3.8 D	2 x 3.0	+ 1.41
Q5	3.8 D	2 x 3.0	- 1.35
Q6	3.8 D	3.0	- 1.89
Q7	3.8 D	3.0	+ 2.17

[1] Assumes P1=+1000 GeV/c, P2=-200 GeV/c, P_{LO}=+150 GeV/c.

The beam spot size and momentum spectrum calculated by TURTLE is shown in Fig. 5. The dump aperture is taken as 2.0 cm x 2.0 cm at a distance of 15M from the tertiary beam production target. This allows a 0.44 μsr solid angle acceptance from the target, adequate for most purposes. this aperture could be stopped down to limit intensity if desired by a collimator slit placed behind the beam dump and before the quadrupole Q6. The aperture of the dump (2.0 cm x 2.0 cm) does not limit the beam envelope for the high momentum tunes as can be seen in Fig. 1.

Tagging of tertiary beam particles is accomplished with 1.0 mm pitch MWPC chambers placed around the quadrupoles Q6, Q7. Except for the fact that a quadrupole rather than a dipole field is used, the method is the same as for tagging the high energy beam. The actual target point is a useful constraint for the tagging. The central trajectory rays have no analyzing power from the quadrupole field, of course, but their momentum is determined from the target position and the B6 dipole sweeping field. Momentum tagging resolution of 1% or so should be possible with reasonable systems. Again, as in the high energy beam case, the spaces between magnets can be used for particle ID devices.

Particle Yields

Test beam flux yields for the design presented in this paper are given in Fig. 6. the particle production data used in calculating the yields are taken by strict energy scaling of the data of Atherton et al[4]. The secondaries as plotted assume a primary beam of 1 TeV protons incident on a 1.0 interaction-length Be production target. Beam transport efficiencies were calculated by TURTLE as noted above. Fluxes are shown by particle type with the assumption that particle ID will allow separation by type in some applications. Calculation of electron and muon yields is beyond the scope of this paper (but could be done with a moderate amount of work by interested parties).

For applications where the particle type doesn't matter, the positive and negative hadrons summed over type are also shown in Fig. 6. Non-interacting and diffraction scattered beam protons are not shown explicitly, but will be large compared to the inelastic particle fluxes shown. Yields of negatives peak at about 200 GeV and drop precipitously above 800 GeV. Fluxes below 10 GeV drop as a result of non-optimum acceptance of the beam transport.

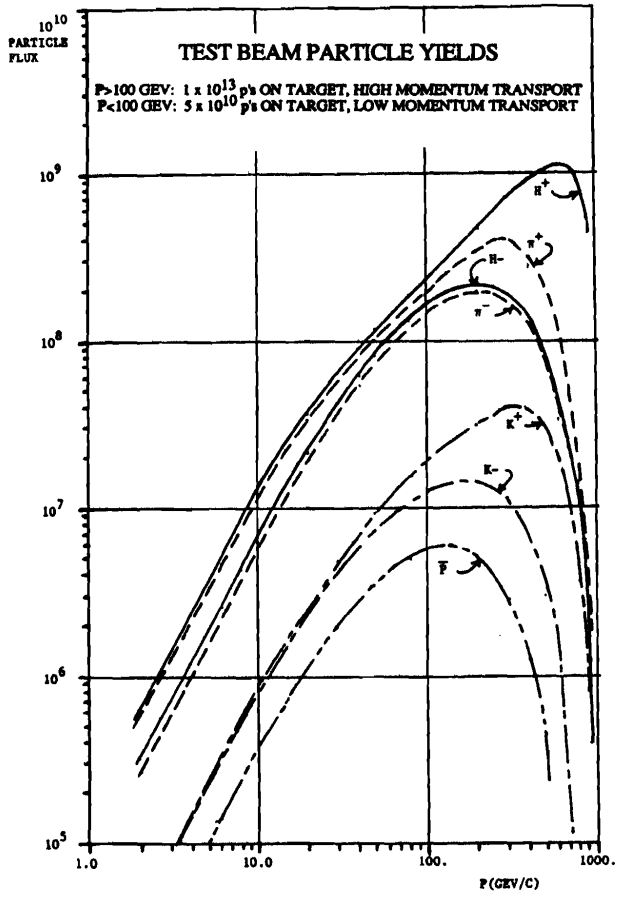

Fig. 6 - Test Beam particle yields from the high and low momentum magnet transports.

Yields for beam energies above 100 GeV assume a primary proton flux of 1.0 x 10^{13} on a one interaction length target plus transport through the high energy beam system. Yields below 100 GeV assume 5.4 x 10^{10} protons incident on the second target station and transport through the low energy system. It is possible to use either transport between about 100 GeV and 150 GeV. Fewer protons are needed for the second system since it has a much larger momentum acceptance and significantly larger solid angle. Beam optical quality is reduced relative to the high energy transport. Both systems have their uses and advantages.

Conventional Construction and Radiation Protection

The beam transport just detailed is based on underground beam handling and target enclosures of concrete construction overlain with mounded earth and connected by buried steel vacuum pipes for beam transport. The beam elevation is expected to lie about 3M below the surface. In this geometry, the radiation shielding is achieved in an effective and economical manner.

As noted above, radiation safety and radiation protection are paramount concerns for facilities of this type. Putting the beam transport below ground is a generally good idea for safe containment of radiation under various accident conditions as well as for absorbing high energy muons which are always present at some level. Activation of soil and groundwater can be controlled by the use of local steel shielding at high loss points such as target stations and dumps. We assume such a scheme in this design.

Finally, the Test Hall is assumed to be a building with a high bay area extending to about 6M below ground level, with counting houses to the sides at ground level. The high bay extends about 10M above ground level as a normal steel framed industrial structure. The details are not part of this paper but are noted in the SSC CDR[3].

References

[1]M. Harrison and T. E. Toohig, 'A Possible Reconfiguration of the SSC Test Beams Facility Providing 1 TeV and 20 TeV Proton Targeting and the Possibility of High Intensity Neutrals', SSC Snowmass Summer Study Proceedings, 1986.

[2]Tevatron II Design Handbook Vols. I and II, Fermilab 1986.

[3]SSC Conceptual Design Report, SSC-SR-2020, April 1986.

[4]H.W. Atherton, et al, 'Precise Measurement of Particle Production by 400 GeV/c Protons on Beryllium Targets', CERN 80-07, (1980).

[5]D. Carey, K. L. Brown, and Ch. Iselin, 'DECAY TURTLE, A Program for Simulating Charged Particle Beam Transport Systems, Including Decay Calculations', SLAC - 246, March 1982.